IEEE Access
Multidisciplinary | Rapid Review | Open Access Journal

Received March 1, 2021, accepted March 11, 2021, date of publication March 17, 2021, date of current version March 23, 2021.

Digital Object Identifier 10.1109/ACCESS.2021.3066281

MPPT Algorithm Based on Artificial Bee Colony for PV System

CATALINA GONZÁLEZ-CASTAÑO[1], CARLOS RESTREPO[2], SAMIR KOURO[3], (Senior Member, IEEE), AND JOSÉ RODRÍGUEZ[1], (Life Fellow, IEEE)

[1]Department of Engineering Sciences, Universidad Andres Bello, Santiago 7500971, Chile
[2]Department of Electromechanics and Energy Conversion, Universidad de Talca, Curicó 3349001, Chile
[3]Department of Electronics Engineering, Universidad Técnica Federico Santa María, Valparaiso 2390123, Chile

Corresponding author: Carlos Restrepo (crestrepo@utalca.cl)

This work was supported in part by the Chilean Government through the Project Conicyt Agencia Nacional de Investigación y Desarrollo (ANID)/Fondo Nacional de Desarrollo Científico y Tecnológico (FONDECYT) under Grant 1191680, in part by the Advanced Center of Electrical and Electronic Engineering (AC3E) under Grant ANID/FB0008, in part by the Solar Energy Research Center (SERC Chile) under Grant ANID/FONDAP/15110019, in part by the ANID/Programa de Investigación Asociativa (PIA)/ACT192013, and in part by the ANID/FONDECYT/1210208.

ABSTRACT Energy structures from non-conventional energy source has become highly demanded nowadays. In this way, the maximum power extraction from photovoltaic (PV) systems has attracted the attention, therefore an optimization technique is necessary to improve the performance of solar systems. This article proposes the use of ABC (artificial bee colony) algorithm for the maximum power point tracking (MPPT) of a PV system using a DC-DC converter. The procedure of the ABC MPPT algorithm is using data values from PV module, the P-V characteristic is identified and the optimal voltage is selected. Then, the MPPT strategy is applied to obtain the voltage reference for the outer PI control loop, which in turn provides the current reference to the predictive digital current programmed control. A real-time and high-speed simulator (PLECS RT Box 1) and a digital signal controller (DSC) are used to implement the hardware-in-the-loop system to obtain the results. The general system does not have a high computational cost and can be implemented in a commercial low-cost DSC (TI 28069M). The proposed MPPT strategy is compared to the conventional perturb and observe method, results show the proposed method archives a much superior performance.

INDEX TERMS Maximum power point tracking, photovoltaic system, artificial bee colony, hardware in the loop testing.

ABBREVIATION

Term	Description
ABC	Artificial bee colony algorithm.
ACO	Ant colony optimization.
ADE	Adaptive differential evolution.
ANFIS	Adaptive neuro-fuzzy inference system.
ANNs	Artificial neural networks.
BA	Bat algorithm.
BI	Bio-inspired methods.
COA	Coyote optimization algorithm.
DSC	Digital signal controller.
ESC	Extremum-seeking control.
FL	Fuzzy logic algorithm.
FPA	Flower pollination algorithm.
FPGA	Field-programmable gate arrays.
GA	Genetic algorithm.
HIL	Hardware-in-the-loop.
INC	Incremental conductance algorithm.
MOA	Moth-flame optimization algorithm.
MPP	Maximum power point.
MPPT	Maximum power point tracking.
PCC	Predictive digital current programmed control.
PGJAYA	Performance-guided JAYA.
PSO	Particle swarm optimization.
P&O	Perturb and observe algorithm.
PSO	Particle swarm optimization.
PV	Photovoltaic.

The associate editor coordinating the review of this manuscript and approving it for publication was Shihong Ding.

I. INTRODUCTION

The high use of generators, loads and storage systems to the main grid, turns the energy transformation more challenging, and so control objectives are demanded according to the needs of modern electrical systems [1], [2]. This is the case,

TABLE 1. Soft computing MPPT methods.

MPPT algorithm	Ref.	MPPT reference output (f_{samp})			Converter (f_s)		Steady-state oscillations	MPPT Efficiency	Tracking Speed	Implementation complexity	Controller Cost	Experimental results
		Duty cycle	Voltaje	Current	Boost	Buck-boost						
ADE	[12]	(NF)				(25 kHz)	No	H	M	M	H	No
FPA	[13]	(3.3 Hz)			(10 kHz)		No	H	H	H	M	Yes
MFOA	[14]	(NF)			(50 kHz)		No	H	L	H	M	Yes
GA	[15]			(NF)	(20 kHz)		No	H	H	M	H	Yes
PGJAYA	[16]		(3.3 Hz)		(20 kHz)		No	M	M	M	M	Yes
COA	[17]	(NF)			(NF)		No	L	M	M	NF	No
FL	[18]	(NF)			(Variable)		No	H	H	H	H	No
ANNs	[19]		(NF)		(NF)		No	H	H	H	H	No
PSO	[20]	(5 Hz)			(50 kHz)		Yes	L	H	H	M	Yes
ACO	[21]	(NF)				(10 kHz)	No	H	H	H	H	Yes
BA	[22]	(NF)				(50 kHz)	No	H	H	H	H	Yes
ABC	[23]	(20 Hz)			(20 kHz)		Yes	H	M	H	H	Yes
This work	[-]		(10 Hz)		(25 kHz)		No	H	H	H	L	Yes

f_{samp}: Updating frequency of the MPPT algorithm, f_s: Converter switching frequency, NF: Information not found, H: High, M: Medium, L: Low.

for instance, of grid-connected systems such as renewable energy [3]–[5]. Numerous works have addressed researches to obtain high efficiency in PV systems using an optimizer known as maximum power point tracking (MPPT) [6]. Typically, the maximum power point (MPP) is achieved by adjusting some parameters (current, voltage or conductance) of the PV array using a DC–DC converter [7]–[9]. Conventionally, MPPT algorithm is based on linear controllers such as perturb and observe (P&O) and extremum-seeking control methods (ESCs) [10], [11]. However, this linearized control structure has an inherent medium dynamic response and low yields.

In recent years, bio-inspired (BI) methods, such as swarm intelligence algorithms, have gained increased attention as powerful optimization algorithms for solving complex problems and providing optimum solutions. Some soft computing algorithms have been used to adjust the gains of a proportional-integral control for MPPT of PV systems and show a high performance [24]–[26]. The comparison of MPPT methods based on soft computing algorithms for different control variables and DC-DC converters are shown in Table 1. Most of the soft computing MPPT methods have been implemented in expensive and high processing devices, unlike this proposed work.

Among the bio-inspired methods, this article is focused on the ABC algorithm, which is a swarm intelligence algorithm that is widespread and inspired by the social behavior of honeybees [27]. The ABC algorithm has been widely applied in distinct fields of electrical engineering such as: in fault diagnosis [28], [29], optimized PID controller design [30], optimal power dispatching [31], automatic voltage regulator system [32], MPPT power extraction [23], [33],and antenna design [34], [35].

In Table 1, the work is presented [23] which is an ABC MPPT algorithm available in the literature which has great differences regarding the proposed one in this article. The work presented in [23], the ABC MPPT algorithm estimates the duty cycle for a boost converter switching at 20 kHz. However, the updating of this duty cycle is performed each 20 Hz which corresponds to a thousand time less than the converter switching frequency. There are two reasons for this low updating control law. The first one, the oscillation in the converter's current and voltage waveforms at each new duty cycle updating, which requires a relevant stabilization time before using the algorithm again. The second one, the computational cost of using the ABC MPPT algorithm which does not allow to increase the sampling frequency due to the hardware limitation. The final results of the limitations presented in [23] are relevant noise in the converter signals in steady-state and a poor dynamic of the MPPT tracking under irradiance changes. These problems can be solved by decoupling the dynamics of the MPPT and the control of the converter by means of a fast current loop as it is proposed in this article. But to do so, a new ABC MPPT algorithm is required to estimate not the converter duty cycle but its input voltage

reference. However this is a great challenge that is addressed in this article as the converter will operate at a high frequency under a low-cost microcontroller. Besides, the MPPT algorithm in [23] is compared to the particle swarm optimization (PSO) based on the MPPT algorithm, showing improved performance, although the implementation of the PSO MPPT algorithm is complex and has a very expensive cost [36]. In order to foster the acceptance of new control methods by commercial devices, it is mandatory to evaluate the merits of intelligent algorithms suitable for low-cost embedded board and to fairly compare their performance against established solutions of low-computational cost. A well-known MPPT method, already used in commercial products, is the perturb and observe strategy [37]. ABC MPPT algorithms seen in [23] and [38] have not been compared to well-known and established MPPT techniques with a low-cost computational cost unlike the proposed technique.

Therefore, this article proposes a novel MPPT method based on the ABC algorithm. The ABC algorithm is used to identify the P-V characteristic of a solar module. Then, a search of the optimal voltage reference for the selected P-V characteristic is realized. The main advantages of using the ABC algorithm are: excellent tracking capability with high efficiency, parameters knowledge is not necessary and the increment of simplicity. Therefore, the ABC algorithmic is suitable to achieve a digital implementation using a low-cost (digital signal controller) DSC. The MPPT is implemented with a DC-DC boost converter, the PV module and the DC-DC converter are modeled with a real-time and high-speed simulator (PLECS RT Box 1). The MPPT algorithm is developed using C language and programming a commercial low-cost DSC (TI 28069M). The different control loops of the system are evaluated by hardware-in-the-loop (HIL) tests. In addition, another contribution of this work is the performance comparison of the ABC MPPT algorithm and the conventional perturb and observe strategy under a temperature and irradiance profile. Based on this state-of-the-art review, the main contributions of this article are the following.

- Provide a novel method to determine the MPP of the PV module based on ABC algorithm without oscillations around the MPP in steady state. The training phase of the ABC algorithm only requires the 10% of the data of the P-V characteristic curves (at different levels of irradiation and ambient temperature) given by the manufacturer of the PV module.
- The design of two nested control loops with a current (inner loop) controller and a voltage (outer loop) controller along with the ABC MPPT algorithm allows to regulate the output voltage PV module under irradiance and ambient temperature conditions. Each of the proposed controllers ensure fast tracking of the control set-points, low steady state error under demanding tests that include system start-up, irradiance variations and irradiance and ambient temperature profile. The implementation of these loops allows independent and fast dynamic response of the system.
- The implementation of the proposed MPPT algorithm and the double loop control of the DC-DC boost converter in a commercial low-cost DSC to be accepted by commercial devices.
- The proposed MPPT method is tested by simulation and Hardware in the loop to demonstrate its feasibility and superior robustness to obtain the MPP of the PV module compared to the conventional P&O method, which has been a well-establish method and available in commercial products.

The remainder of this article is structured as follows: Section II outlines the system description. Section III describes the proposed MPPT approach. Section IV presents the simulated and hardware-in-the-loop results. Finally, the concluding remarks are drawn in Section V.

II. PV SYSTEM DESCRIPTION

The PV module in Figure 1 supplies voltage and current, converting incident solar radiation into electrical energy through the photoelectric effect, to charge a battery through the DC-DC converter. The MPPT control and double loop algorithms are illustrated in Figure 1. The non-linear V-I characteristic and P-V of the BP365 are shown in Figure 2 for different irradiance and temperatures which include 0°C, 25°C and 50°C. This PV module is modelled for PLECS simulations and is presented in [39].

In this work, a boost converter is the selected topology to be used as DC-DC converter. Figure 1 shows the topology of the boost converter. Then, the following system of differential equations for the boost converter is obtained:

$$\frac{di_L(t)}{dt} = \frac{v_g - (1-u)v_o}{L} \tag{1}$$

$$\frac{dv_o(t)}{dt} = \frac{-v_o}{R_L C} + \frac{(1-u)i_L}{C}, \tag{2}$$

with i_L being the inductor current, v_o the output voltage and u the control variable $\in \{0, 1\}$. The duty cycle for the boost converter is:

$$\bar{u} = 1 - \frac{\bar{v}_g}{\bar{v}_o}. \tag{3}$$

A. PREDICTIVE DIGITAL CURRENT PROGRAMMED CONTROL

The predictive digital current programmed control (PCC) is presented in [40], [41]. The law control for this technique can be presented taking into account the slopes for inductor current of the boost converter seen in Table 2, and is expressed in discrete form, as follows:

$$u[n+1] = -u[n] + \frac{1}{(m_1+m_2)T} e_i[n] + 2\frac{m_2}{m_1+m_2}, \tag{4}$$

And the control law for the boost converter is:

$$u[n+1] = -u[n] + \frac{L}{v_o[n]T} e_i[n] + 2\left(1 - \frac{v_g[n]}{v_o[n]}\right). \tag{5}$$

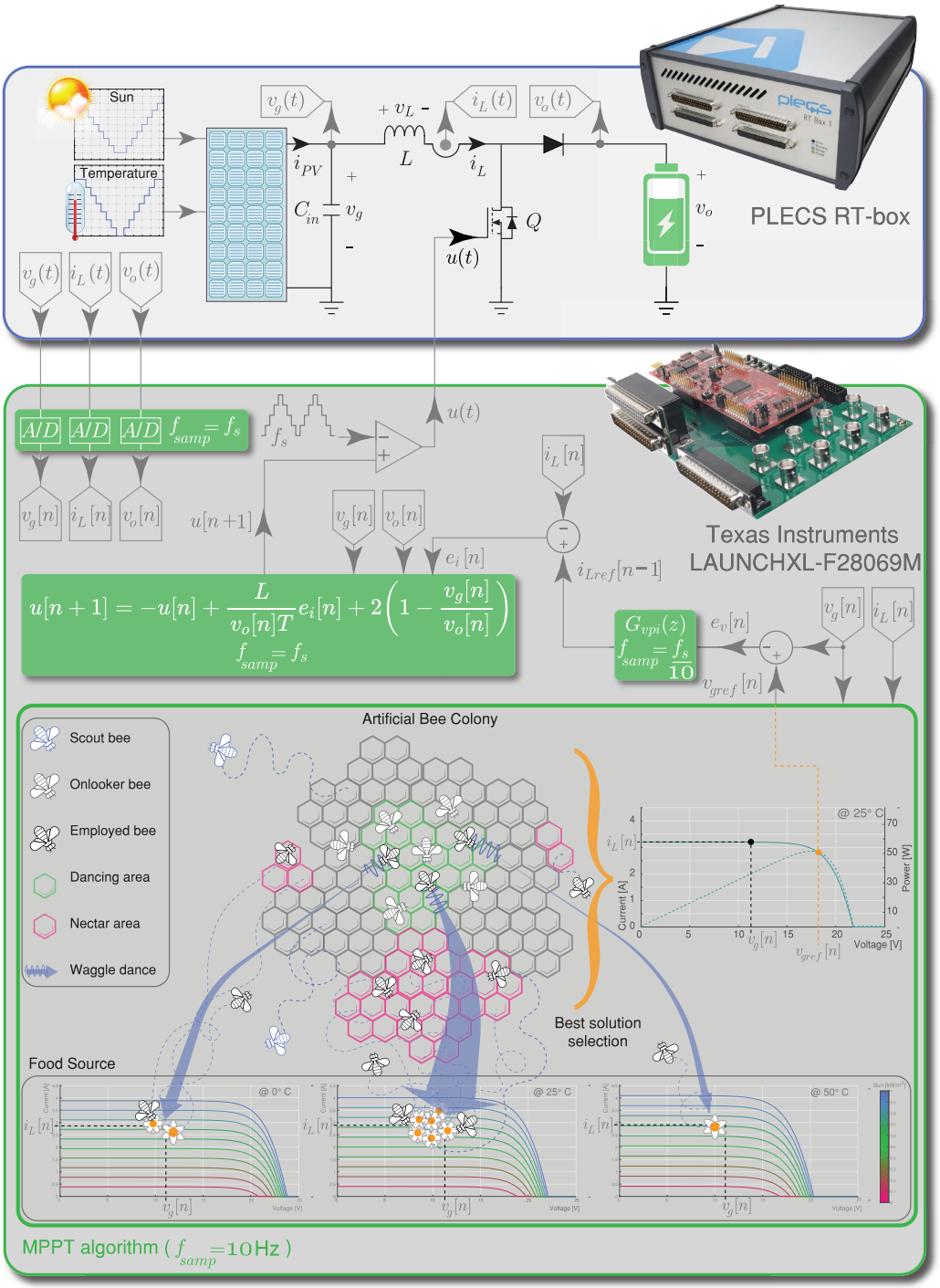

FIGURE 1. Block diagram of the digital controller for the MPPT of the boost converter.

B. DISCRETE-TIME PI VOLTAGE CONTROL

A proportional-integrator controller is used as external loop to regulate the input voltage of boost converter v_g, where the controller transfer function can be expressed in the z domain using the forward Euler method, as follows:

$$G_{vpi}(z) = K_{pv} + \frac{K_{iv} T_{samp}}{z - 1}, \tag{6}$$

where $T_{samp} = 1/f_{samp}$. Being

$$K_{pv} = 2\pi \; C_{in} f_c \tag{7}$$

and

$$K_{iv} = \frac{K_{pv}}{T_i}, \tag{8}$$

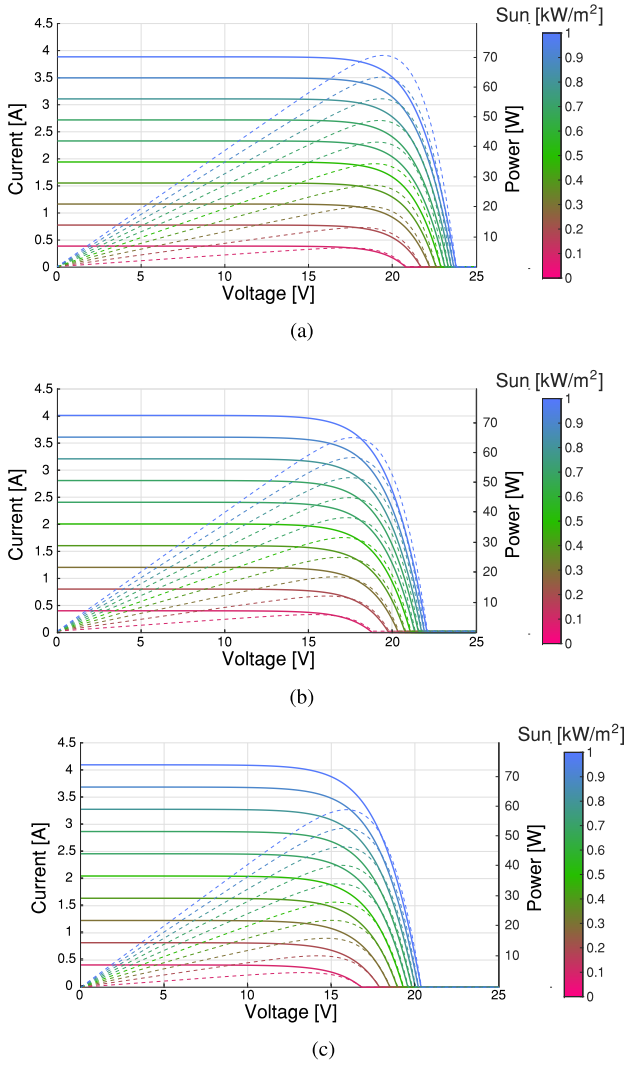

FIGURE 2. Curve PV module I-V characteristic (a) 0°C temperature, (b) 25°C and (c) 50°C.

TABLE 2. Slope of the inductor current waveform.

Converter	m_1	$-m_2$
Boost	$\frac{v_g}{L}$	$\frac{v_g - v_o}{L}$

where, C_{in} is the input capacitor, and the value of the crossover frequency (CF) for the voltage loop (f_c) should be lower than the CF for the current loop. The location of the PI zero should be lower than f_c ($1/(2\pi T_i) < f_c$).

III. ABC MPPT ALGORITHM

The artificial bee colony (ABC) is based on a meta-heuristic algorithm that was introduced for solving multidimensional optimization problems [23]. The algorithm is based on the model proposed in [42], [43] for the foraging behavior of honey bee colonies. A swarm is a set of honey bees which can

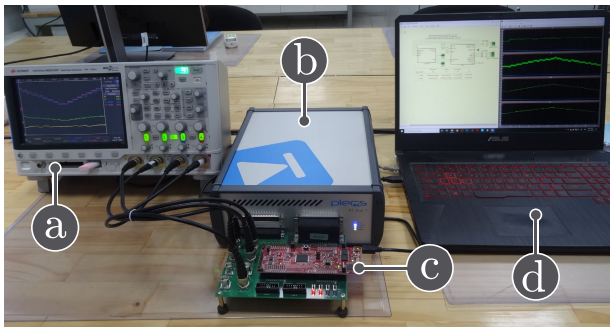

FIGURE 3. Hardware in-the-loop experimental setup: (a) oscilloscope, (b) PLECS RT-box, (c) Texas Instruments LAUNCHXL-F28069M, (d) Laptop.

successfully accomplish tasks through social cooperation. In the ABC algorithm, there are three types of bees: employed bees, onlooker bees, and scout bees as shown in Figure 1. The employed bees search around the food source for pollen and nectar, in the case of the proposed algorithm, this corresponds to the data-set of the P-V characteristic curves at different temperatures shown in Figure 2. The employed bees have the information of the actual operation point of the PV module, which corresponds with the current (i_L[n]) and voltage (v_g[n]), to search into the food source for nectar and pollen. The employed bee shares this information, the food location, with the onlooker bees, by means of a waggle dance in the bee colony (distance, direction and the profitability). Then, the onlooker bees sort out the best food sources, from all those found by the employed bees. The onlooker bee has the task of evaluating the received food information from all employed bees, and picks out the food source depending on the probability related to its amount of nectar. An employed bee becomes a scout bee if the food source is depleted, then it starts to search for new food sources in a random manner, with no previous experience. If the bee finds a new source, and this new source has an higher amount of food than the last memorized, the bee remembers only the location of the new found and better food source, erasing the other one from its memory. Finally, the better solution determines the curve of all the data-set with the higher probability of an equivalent operation point. Once this curve is known, by means of a lookup table, the value of the voltage ($v_{gref}[n]$) at the maximum power can be found. Therefore, the ABC system combines local search methods, carried out by employed and onlooker bees, with global search methods, managed by onlookers and scouts, attempting to balance exploration and exploitation process.

To implement the ABC MPPT algorithm, a data-set of the P-V characteristic curves shown in Figure 2, are required to generate the maximum possible power solutions. Each solution for the voltage reference is produced defining a vector with the possible values for the voltage of the PV module

$$\mathbf{V_g} = \{v_{g1}, v_{g2}, v_{g1}, \ldots, v_{gi}\} \tag{9}$$

and v_{gi} represents the i^{th} solution. The probability for the powers of all the characteristics curves corresponding to the

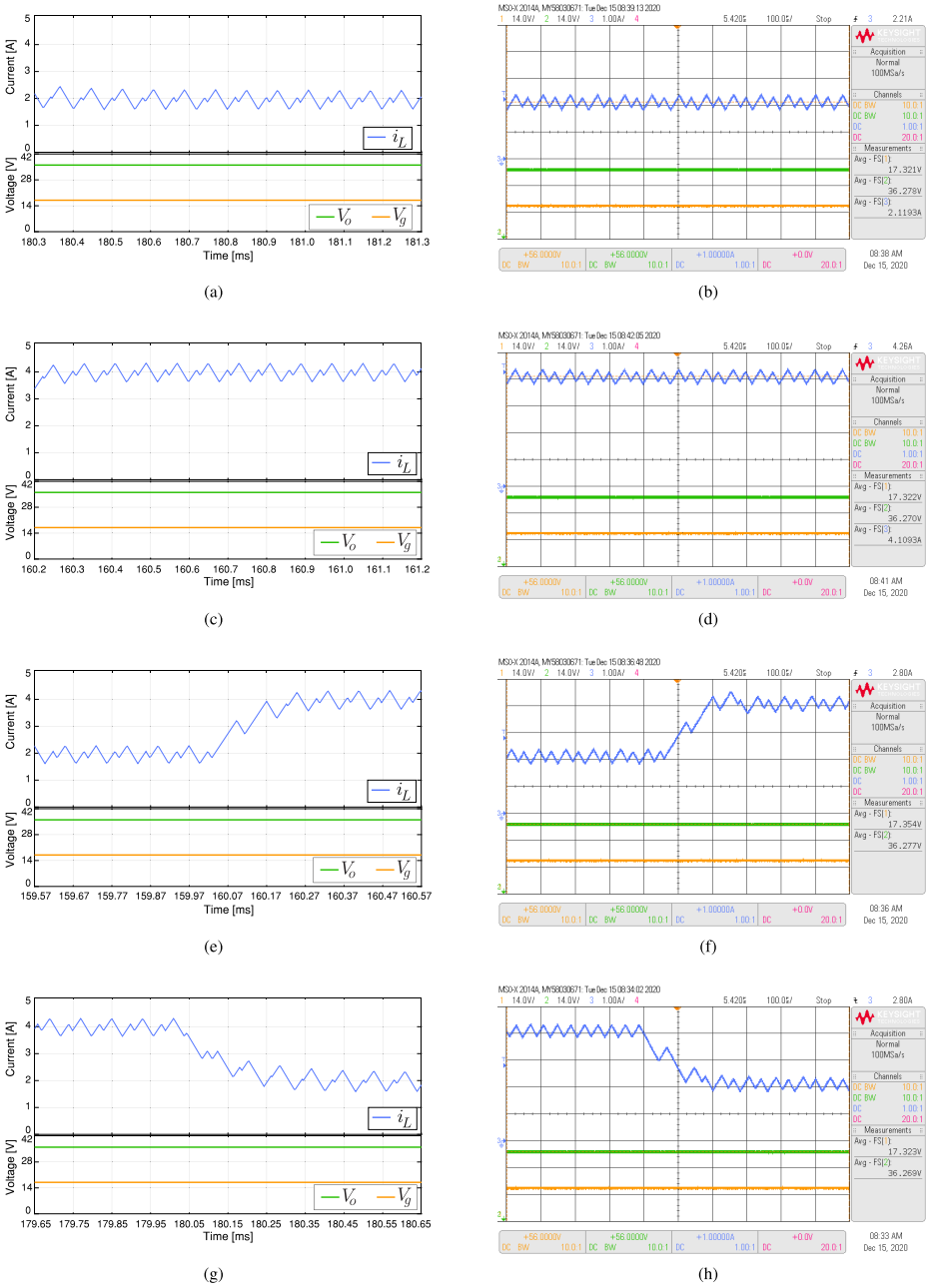

FIGURE 4. Simulated (a), (c), (e), (g) and experimental (b), (d), (f), (h) responses of the predictive digital current input control when the reference i_{ref}: (a,b) is equal to 2 A, (c,d) is equal to 4 A, (e,f) changes from 2 A to 4 A, and (g,h) from 4 A to 2 A. The converter is operating with an input voltage $V_g = 17$ V and an output voltage $V_o = 36$ V). CH1: V_g (14 V/div), CH2: V_o (14 V/div), CH3: i_L (1A/div) and a time base of 100 μs.

input voltage $v_g[n]$ are calculated as [44]:

$$\mathbf{P} = \frac{P_{pv_Q}}{\sum_{Q=1}^{N} P_{pv_Q}} \tag{10}$$

Therefore, $\mathbf{P}$ contains the N probabilities of all characteristics curves corresponding to a sample voltage $v_g[n]$. To calculate the probability function (10), a new solution $newv_g$ is generated using [44]:

$$newv_g = v_{gi} + \phi_i(v_{gi} - v_g) \tag{11}$$

where ϕ_i is a random number between $[-1,1]$. Then, a local searching around the chosen $newv_g$ is realized, which depends on the calculated probability $\mathbf{P}$ and the its actual probability power $P_a = P_{pv}[n]/\sum_{Q=1}^{N} P_{pv_Q}$. The current operating curve of the PV module is etermined by the position of the value of the probability $\mathbf{P}$ nearest to the probability

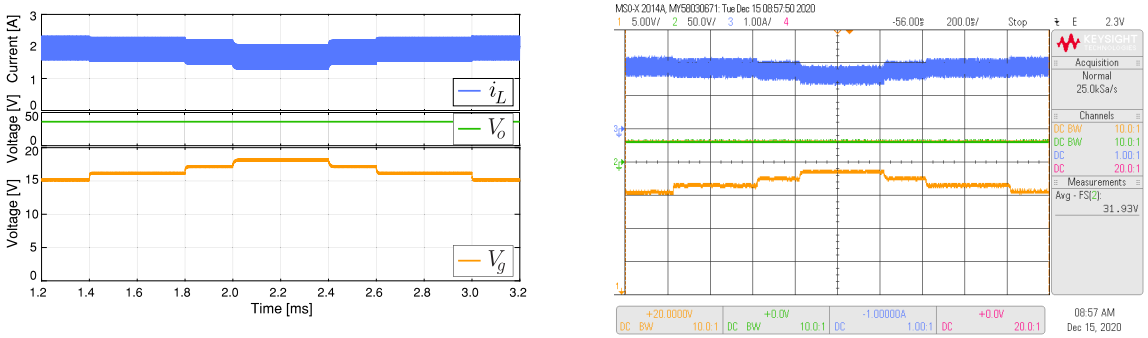

FIGURE 5. Simulated (a) and experimental (b) responses of the double loop using predictive digital current control when the reference v_{ref} changes with steps of 1 V between 15 V to 18 V while the output voltage ($V_o = 36$ V) ensures a boost operation. CH1: v_g (5 V/div), CH2: V_o 50 V/div), CH3: i_L (1A/div) and a time base of 200 ms.

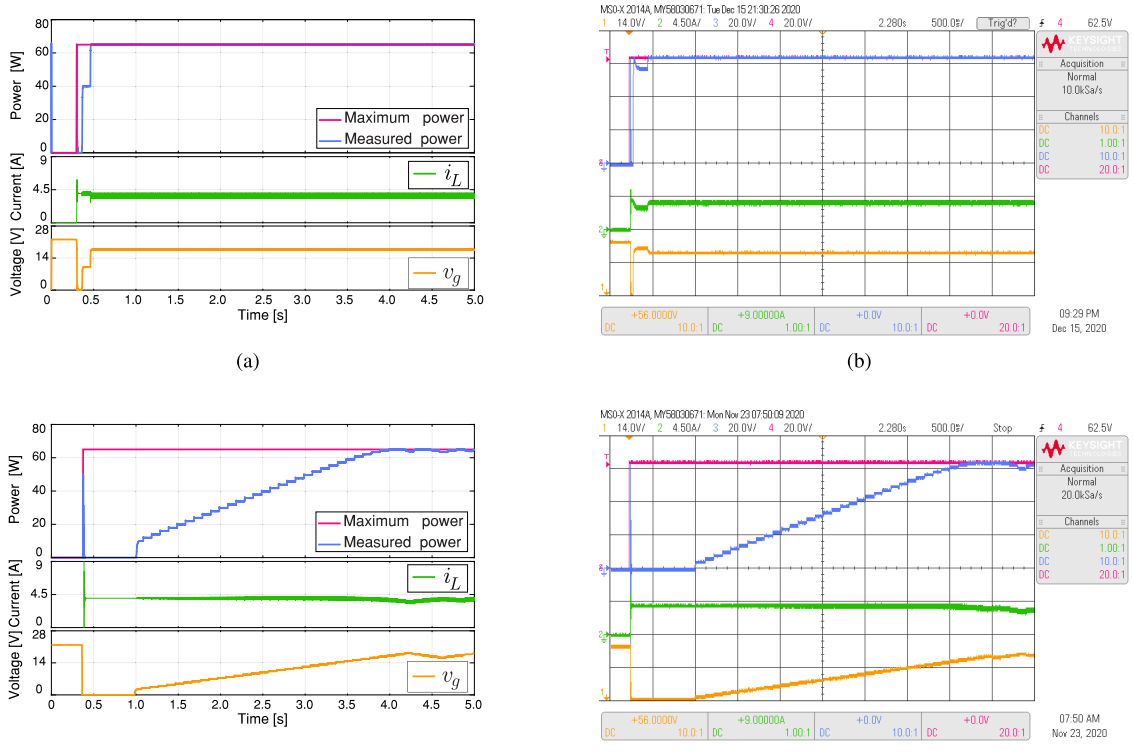

FIGURE 6. Simulated (a), (c) and experimental (b), (d) dynamic behavior of the MPPT algorithms during system start-up with an irradiance of 1000 W/m^2 and an output voltage $V_o = 36$ V. The proposed MPPT algorithm (top) is compared with perturb and observe (P&O) based MPPT algorithm (bottom). CH1: v_g (14 V/div), CH2: i_L (4.5 A/div), CH3: Maximum power (20 W/div), CH4: Measured power (20 W/div) and a time base of 500 ms.

P_a. Once the operating curve is determined, it is possible to establish the maximum voltage of each curve, and to set the voltage V_m for maximum power P_m. The ABC MPPT algorithm is executed when changes of power greater than or equal to reference $\Delta P(\%)$ occur [23], so:

$$\frac{\left|P_{pvnew} - P_{pvlast}\right|}{P_{pvlast}} \geq \Delta P_{pv}(\%), \tag{12}$$

where P_{pvnew} is the actual power measurement and P_{pvlast} is the previous power measurement. Therefore, the search process has to restart whenever the weather conditions change. In the ABC algorithm, the number of candidate solutions is equal to the number of employed and onlooker bees. During this search process, each employed bee produces a new solution $newv_g$ using (11), and calculates the probability values $\mathbf{P}$. Then, the employed bees share the information of their food sources with the onlooker bees through waggle

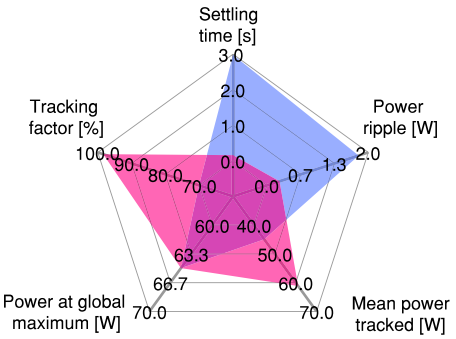

Criteria	P&O	ABC
Settling time [s]	2.98	0.16
Power ripple [W]	1.81	0.25
Mean power tracked [W]	44.93	61.16
Power at global maximum [W]	64.98	64.98
Tracking factor [%]	70.08	98.41

FIGURE 7. Comparative analysis of the MPPT methods during the star-up.

dances. Each onlooker bee selects a solution v_g depending on $\mathbf{P}$ and P_a, if there is an abandoned solution for the scout bee, the replacement with the new solution is be randomly made. Finally, the memorization of the best voltage reference v_{gref} is achieved. The proposed method is described in Figure 1.

IV. RESULTS

In this section, PLECS simulations and hardware in the loop (HIL) tests are run to assess the effectiveness of the ABC MPPT algorithm using a DC-DC boost converter. The PV module and the boost converter are implemented in PLECS RT Box 1, where the sampled time to model the converter is 3 μs. The values of the boost converter components are: $L = 800$ μH, $C_{in} = 88$ μF, switching frequency $f_s = 25$ kHz and $V_o = 36$ V. The MPPT algorithms and the different controls that integrate the PV global system control scheme, as shown Figure 1, are implemented using TI 28069M LaunchPad, which is a low cost Texas Instrument microcontroller.

The HIL setup is shown in Figure 3, where the evaluation kit, a TI 28069M LaunchPad (the red board), is connected to the RT Box via an RT Box LaunchPad Interface (the green board). The proposed MPPT method is compared with P&O algorithm. The PV module used in the simulation is the BP365 65W, and the electrical characteristic is presented in Table 3.

A. INNER LOOP CURRENT CONTROL RESULTS

The current loop time domain responses for the inductor current of the boost converter are shown in Figure 4. The signals sampled for the control are v_g, v_o and i_L. The sampling time is 40 μs. The current reference has been changed from

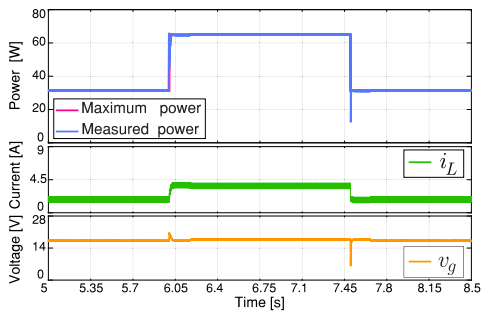

(a)

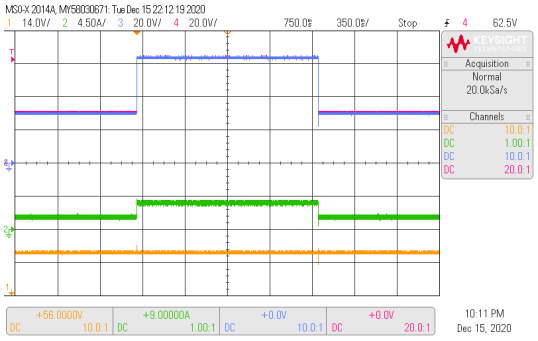

(b)

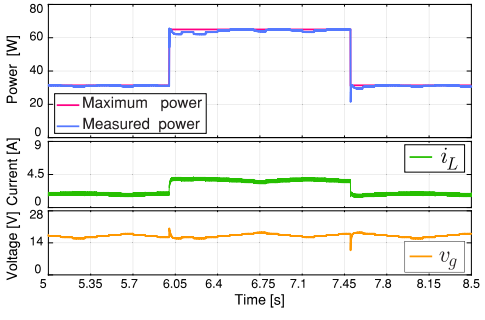

(c)

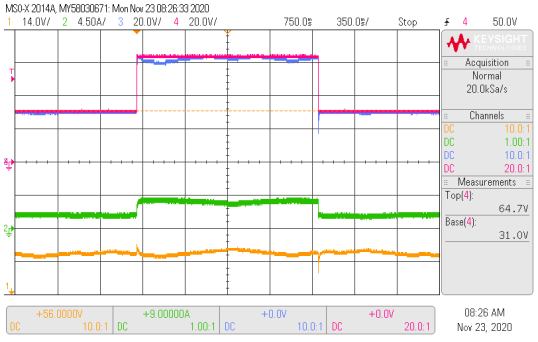

(d)

FIGURE 8. Simulated (a), (c) and experimental (b), (d) dynamic behavior of the MPPT algorithms dealing with sudden changes in irradiance between 1000 W/m^2 and 500 W/m^2 and vice versa. output voltage $V_o = 36$ V. The proposed MPPT algorithm (top) is compared with perturb and observe (P&O) based MPPT algorithm (bottom). CH1: v_g (14 V/div), CH2: i_L (4.5 A/div), CH3: Maximum power (20 W/div), CH4: Measured power (20 W/div) and a time base of 350 ms.

TABLE 3. Electrical characteristics of Pv module BP 365.

Electrical parameters	Value
Maximum power P_{max}	65 W
Voltage at maximum power V_{mp}	17.6 V
Current at maximum power I_{mp}	3.69 A
Short-circuit current I_{sc}	3.99 A
Open-circuit voltage V_{oc}	22.1 V
Temperature coefficient of short-circuit current	(0.065 ± 0.015) %/°C
Temperature coefficient	$-(80 \pm 10)$ mV/°C

2 A to 6 A and back to 2A. The input voltage is set in 17 V, and the output voltage is $V_o = 36$ V. The transitions during reference changes are smooth, without overshoot and settling times near to 150 μs. The simulated results are in good agreement with HIL results. As shown, the output current is well regulated. The controlled current adequately follows the current reference at all times from the steady–state to the variations in the current reference. Thus, the current control performance during current step reference change is validated.

B. DOUBLE LOOP RESULTS

Voltage reference variations from 15 V to 18 V with a step between variations of 1 V were considered for external loop validation. Simulated and HIL test responses are shown in Figure 5. These voltage reference values are in accordance with the voltage for maximum power, as can be observed in Figure 2. The selected crossover frequency (CF) corresponds to $f_c = 500$ Hz which allows the proportional gain calculation according to (7). The location of the PI zero of equation (8) is lower than f_c $(1/(2\pi T_i) < f_c)$ whereby a $T_i = 3.18 \times 10^{-3}$ s was selected. In Figure 1 the voltage regulator ($G_{vpi}(z)$) calculates the inductor current reference every 400 μs.

This experiment is performed at a fixed temperature of 25 ° and a fixed irradiance of 600 W/m^2 for the PV module. As can be observed in Figure 5, the voltage reference is accurately tracked and the current transitions caused by the voltage changes are smooth.

C. COMPARISON OF MPPT METHODS RESULTS

This comparison is performed with the classical P&O algorithm approach. The MPPT algorithms are implemented to provide a new voltage reference for the voltage loop, every 100 ms, as shown in Figure 1 for the MPPT algorithm block. For the ABC MPPT, $\Delta P(\%)$ is set to 2%. The parameters of the ABC algorithm have 33 places of food sources and an a beehive composed by 15 onlooker bees and 15 employed bees. The challenge of the proposed ABC MPPT method is its implementation in a low-cost DSC due to the fact that it is a strategy with high computational requirements. According with Figure 1 in the DSC, the inner current loop is updating at 25 kHz, the outer voltage loop is calculating at 2.5 kHz and the MPPT strategy is computing at 10 Hz. These scale time differences between the systems are challenging but at

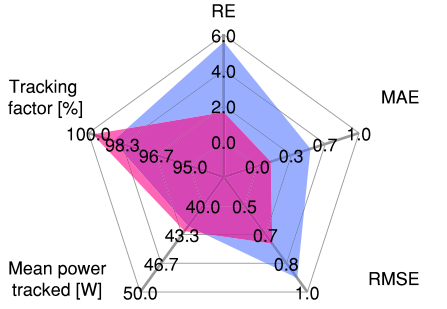

Criteria	MPPT algorithm P&O	ABC
RE	5.598	1.65
MAE	0.521	0.13
RMSE	0.919	0.72
Mean power tracked [W]	42.38	42.94
Tracking factor [%]	98.84	99.8

FIGURE 9. Comparative analysis of the MPPT methods under irradiation variations.

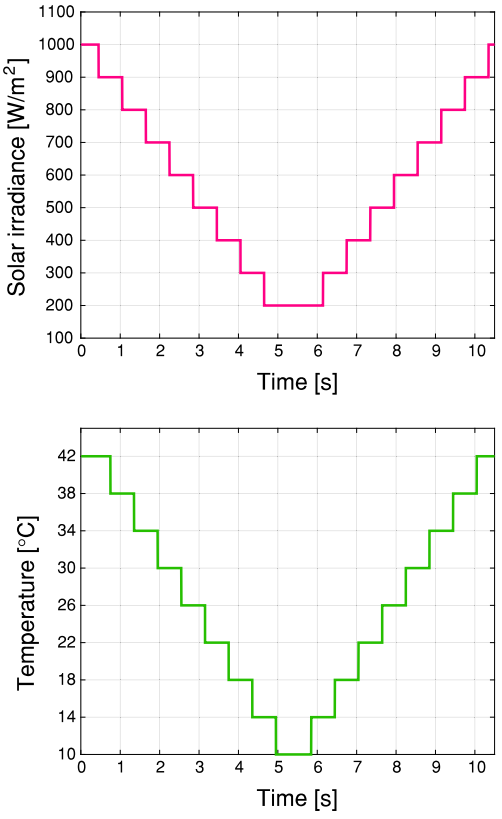

FIGURE 10. Irradiance and temperature profile.

the same time advantageous to implement a MPPT based on a finite-state machine. In this case, the total code of the ABC MPPT method is divided into 30 states that are calculated each 3.3 ms. This way, the MPPT strategy is computing at 10 Hz which allows fair comparisons with other methods. In addition, the small pieces of code that composes each state

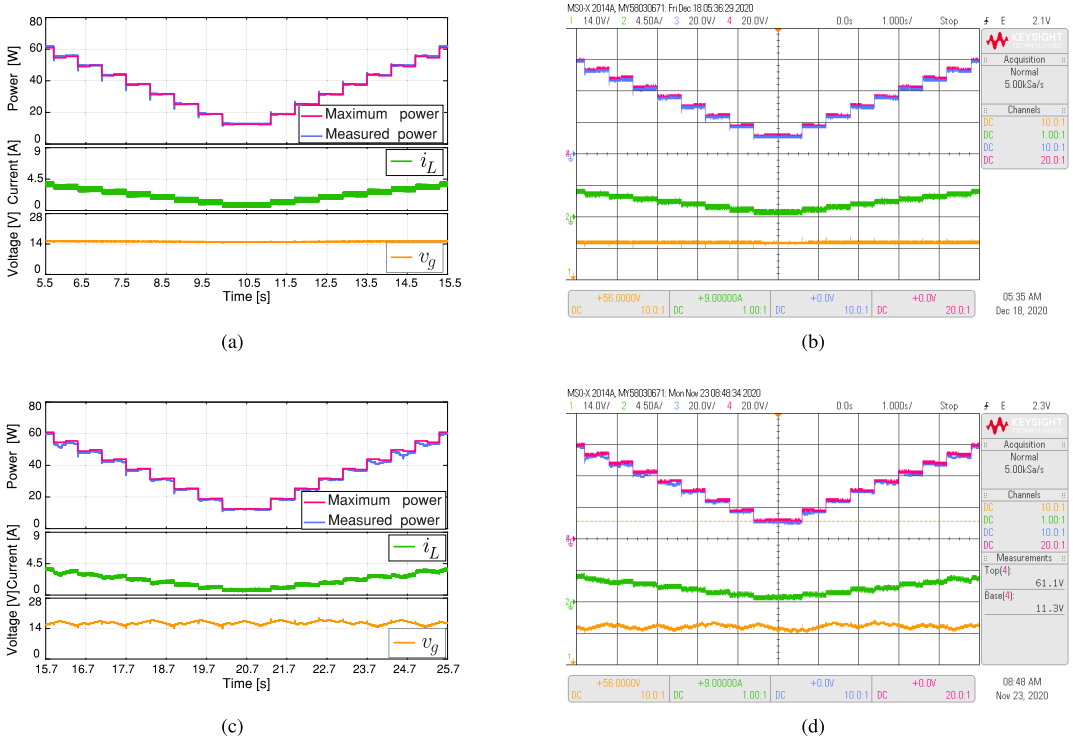

FIGURE 11. Simulated (a), (c) and experimental (b), (d) dynamic behavior of the MPPT algorithms dealing with changes in irradiance and temperature according to the profile shown in Figure 10. Output voltage $V_o = 36$ V. The proposed MPPT algorithm (top) is compared with perturb and observe (P&O) based MPPT algorithm (bottom). CH1: v_g (14 V/div), CH2: i_L (4.5 A/div), CH3: Maximum power (20 W/div), CH4: Measured power (20 W/div) and a time base of 1 s.

machine can be computing at each loop iteration together with the voltage and current loops avoiding overcomputation in the low cost DSC. First comparison results are the start-up for the MPPT methods shown in Figure 6. This figure gives the transient behavior from zero current to an equilibrium point corresponding to the maximum power at a fixed irradiance of 1000 W/m^2 and a fixed ambient temperature of 25°C for the PV module. In Figures 6(a) and 6(b) the ABC MPPT reaches the steady state close to 0.16 s while for the P&O method in Figures 6(c) and 6(d) the steady state is reached in around 2.98 s, having the proposed MPPT a faster tracking than the P&O method during system start-up. It is important to note that while the P&O algorithm tracks the maximum power point, an oscillating signal around the maximum is always generated. The proposed MPPT algorithm works at the optimum point and there is no oscillation after it has been tracked. Figure 7 shows a quantitative analysis of the proposed MPPT method and P&O method for the results shown in Figure 6. This values demonstrate a higher performance of the proposed MPPT method in comparison to the P&O method during the start-up, where the ABC MPPT algorithm has a higher tracking factor, the mean power tracked value is close to the power global maximum and the setting times is significantly shorter than the P&O strategy.

The second comparison results are under step irradiation variations from 500 W to 1000 W and return to 500 W with a fixed temperature of 25°C. Figure 8 shows simulated and HIL results of the MPP tracking performance. Figures 8(a) and 8(b) are the results for the ABC MPPT and Figures 8(c) and 8(d) are the results for the P&O algorithm. The overall MPPT tracking efficiency for the P&O method is 97.56 % and for the ABC MPPT, 99.79 %. For the classical P&O method, the PV system always operates in an oscillating mode, as can be observed by the inductor current and input voltage of the converter in Figures 8(c) and 8(d). Figure 9 shows the sensitivity of the algorithms by mean absolute error (MAE), relative error (RE), and root means square error (RMSE) for the results shown in Figure 8. The standard error equations are given in [45]:

$$\mathrm{RE} = \frac{\sum_{i=1}^{m}(P_{pvi} - P_{mpp})}{P_{mpp}} 100\% \tag{13}$$

$$\mathrm{MAE} = \frac{\sum_{i=1}^{m}|P_{pvi} - P_{mpp}|}{m} \tag{14}$$

$$\mathrm{RMSE} = \sqrt{\frac{\sum_{i=1}^{m}(P_{pvi} - P_{mpp})^2}{m}} \tag{15}$$

where P_{pvi} represents the measured power of the PV module, P_{mpp} is the available MPP power of the solar module and m the total number of sampling data. Standard errors values indicate that the performance of the proposed MPPT algorithm has a higher effectiveness to tracking the maximum power point. Therefore, the ABC MPPT method archives a

TABLE 4. General comparison of the MPPT methods.

MPPT algorithm	P&O	ABC
Parameters knowledge	Not necessary	Not necessary
Complexity	Low	Moderate
Oscillation around MPP	Yes	No
Parameter tuning	No	No
Convergence speed	Slow	Fast
Overall efficiency	High	High
Precision	Low	High

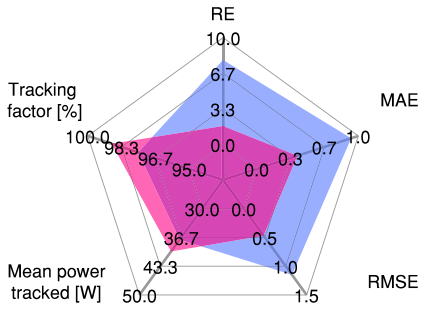

Criteria — MPPT algorithm: P&O, ABC

RE	7.91	1.72
MAE	0.93	0.4
RMSE	1.15	0.47
Mean power tracked [W]	37.17	39.92
Tracking factor [%]	97.52	98.92

FIGURE 12. Comparative analysis of the MPPT methods under irradiation and temperature variations.

much superior performance for abrupt irradiation variations than the classical P&O method.

The third comparison results are under the irradiance and temperature profile shown in Figure 10. This test demonstrates the controller robustness and the ability to keep extracting the maximum power within this abrupt variations. Figures 11(a) and 11(b) for the ABC MPPT present an overall MPPT tracking efficiency of 99.6 % for variations following the profile in Figure 10 while for the P&O method the tracking efficiency is 97 % for Figures 11(c) and 11(d). Moreover, the proposed MPPT does not present oscillations signals (power, current and input voltage) compared with the P&O one. The accuracy of the proposed MPPT method under irradiance and ambient temperature profile (results of Figure 11) is evaluated by using the standard errors (13), (14) and (15), and the scores of mean power tracked and tracking factor as shown Figure 12. This figures revels that the proposed MPPT method has high MPP tracking capability with respect to P&O method. A summary of MPPT techniques comparison is shown in Table 4, where the proposed MPPT is highlighted for its high efficiency and precision, although its complexity is high, it can be implemented in a commercial low-cost DSC as has been demonstrated in this article.

V. CONCLUSION

The artificial bee colony algorithm is proposed in this article to obtain the optimal voltage reference for the outer PI loop to extract the maximum power of a PV system.

The main advantages of this algorithm are: excellent tracking capability with high efficiency, parameters knowledge is not necessary, and increment of flexibility and simplicity, and its fast response due to the implementation of a double loop control with an inner current control ensuring a fast tracking power.

To validate the effectiveness of the ABC algorithm, an RT Box 1 is used to model the power circuit by the PLECS simulation tool. The MPPT algorithm was implemented in a commercial low-cost DSC, using C programming software. The ABC MPPT method provides high efficiency results in comparison to P&O MPPT for constant and varying weather conditions.

Future works will address the combination of the ABC algorithm with a supervising procedure able to deal with multi-peak i-v curves caused by the activation of bypass diodes in partial shadowing operating conditions.

REFERENCES

[1] S. S. Thale, R. G. Wandhare, and V. Agarwal, "A novel reconfigurable microgrid architecture with renewable energy sources and storage," *IEEE Trans. Ind. Appl.*, vol. 51, no. 2, pp. 1805–1816, Sep. 2015.

[2] M. Awais, L. Khan, S. Ahmad, S. Mumtaz, and R. Badar, "Nonlinear adaptive neurofuzzy feedback linearization based MPPT control schemes for photovoltaic system in microgrid," *PLoS ONE*, vol. 15, no. 6, Jun. 2020, Art. no. e0234992.

[3] A. Iovine, S. B. Siad, G. Damm, E. De Santis, and M. D. Di Benedetto, "Nonlinear control of a DC microgrid for the integration of photovoltaic panels," *IEEE Trans. Autom. Sci. Eng.*, vol. 14, no. 2, pp. 524–535, Apr. 2017.

[4] K. Kumar, N. Ramesh Babu, and K. R. Prabhu, "Design and analysis of RBFN-based single MPPT controller for hybrid solar and wind energy system," *IEEE Access*, vol. 5, pp. 15308–15317, 2017.

[5] S. Padmanaban, N. Priyadarshi, M. S. Bhaskar, J. B. Holm-Nielsen, E. Hossain, and F. Azam, "A hybrid photovoltaic-fuel cell for grid integration with Jaya-based maximum power point tracking: Experimental performance evaluation," *IEEE Access*, vol. 7, pp. 82978–82990, 2019.

[6] Y. Wang, Y. Yang, G. Fang, B. Zhang, H. Wen, H. Tang, L. Fu, and X. Chen, "An advanced maximum power point tracking method for photovoltaic systems by using variable universe fuzzy logic control considering temperature variability," *Electronics*, vol. 7, no. 12, p. 355, Nov. 2018.

[7] A. El-Shahat and S. Sumaiya, "DC-microgrid system design, control, and analysis," *Electronics*, vol. 8, no. 2, p. 124, Jan. 2019.

[8] C. González-Castaño, L. L. Lorente-Leyva, J. Muñoz, C. Restrepo, and D. H. Peluffo-Ordóñez, "An MPPT strategy based on a surface-based polynomial fitting for solar photovoltaic systems using real-time hardware," *Electronics*, vol. 10, no. 2, p. 206, Jan. 2021.

[9] C. Restrepo, C. González-Castaño, J. Muñoz, A. Chub, E. Vidal-Idiarte, and R. Giral, "An MPPT algorithm for PV systems based on a simplified photo-diode model," *IEEE Access*, p. 1, 2021.

[10] B. Bendib, H. Belmili, and F. Krim, "A survey of the most used MPPT methods: Conventional and advanced algorithms applied for photovoltaic systems," *Renew. Sustain. Energy Rev.*, vol. 45, pp. 637–648, May 2015.

[11] O. Lopez-Santos, G. Garcia, L. Martinez-Salamero, R. Giral, E. Vidal-Idiarte, M. C. Merchan-Riveros, and Y. Moreno-Guzman, "Analysis, design, and implementation of a static conductance-based MPPT method," *IEEE Trans. Power Electron.*, vol. 34, no. 2, pp. 1960–1979, Feb. 2019.

[12] M. F. N. Tajuddin, S. M. Ayob, Z. Salam, and M. S. Saad, "Evolutionary based maximum power point tracking technique using differential evolution algorithm," *Energy Buildings*, vol. 67, pp. 245–252, Dec. 2013.
[13] J. P. Ram and N. Rajasekar, "A novel flower pollination based global maximum power point method for solar maximum power point tracking," *IEEE Trans. Power Electron.*, vol. 32, no. 11, pp. 8486–8499, Nov. 2017.
[14] J.-Y. Shi, D.-Y. Zhang, F. Xue, Y.-J. Li, W. Qiao, W.-J. Yang, Y.-M. Xu, and T. Yang, "Moth-flame optimization-based maximum power point tracking for photovoltaic systems under partial shading conditions," *J. Power Electron.*, vol. 19, no. 5, pp. 1248–1258, 2019.
[15] S. Hadji, J.-P. Gaubert, and F. Krim, "Real-time genetic algorithms-based MPPT: Study and comparison (theoretical an experimental) with conventional methods," *Energies*, vol. 11, no. 2, p. 459, Feb. 2018.
[16] C. Huang, L. Wang, R. S.-C. Yeung, Z. Zhang, H. S.-H. Chung, and A. Bensoussan, "A prediction model-guided Jaya algorithm for the PV system maximum power point tracking," *IEEE Trans. Sustain. Energy*, vol. 9, no. 1, pp. 45–55, Jan. 2018.
[17] H. H. Mostafa and A. M. Ibrahim, "Performance investigation for tracking GMPP of photovoltaic system under partial shading condition using coyote algorithm," in *Proc. 21st Int. Middle East Power Syst. Conf. (MEPCON)*, Dec. 2019, pp. 34–40.
[18] A. Youssef, M. E. Telbany, and A. Zekry, "Reconfigurable generic FPGA implementation of fuzzy logic controller for MPPT of PV systems," *Renew. Sustain. Energy Rev.*, vol. 82, pp. 1313–1319, Feb. 2018.
[19] S. A. Rizzo and G. Scelba, "ANN based MPPT method for rapidly variable shading conditions," *Appl. Energy*, vol. 145, pp. 124–132, May 2015.
[20] J. Shi, W. Zhang, Y. Zhang, F. Xue, and T. Yang, "MPPT for PV systems based on a dormant PSO algorithm," *Electr. Power Syst. Res.*, vol. 123, pp. 100–107, Jun. 2015.
[21] N. Priyadarshi, V. Ramachandaramurthy, S. Padmanaban, and F. Azam, "An ant colony optimized MPPT for standalone hybrid PV-wind power system with single cuk converter," *Energies*, vol. 12, no. 1, p. 167, Jan. 2019.
[22] K. Kaced, C. Larbes, N. Ramzan, M. Bounabi, and Z. E. Dahmane, "Bat algorithm based maximum power point tracking for photovoltaic system under partial shading conditions," *Sol. Energy*, vol. 158, pp. 490–503, Dec. 2017.
[23] A. S. Benyoucef, A. Chouder, K. Kara, S. Silvestre, and O. A. Sahed, "Artificial bee colony based algorithm for maximum power point tracking (MPPT) for PV systems operating under partial shaded conditions," *Appl. Soft Comput.*, vol. 32, pp. 38–48, Jul. 2015.
[24] S. M. Abd-Elazim and E. S. Ali, "Load frequency controller design of a two-area system composing of PV grid and thermal generator via firefly algorithm," *Neural Comput. Appl.*, vol. 30, no. 2, pp. 607–616, Jul. 2018.
[25] A. S. Oshaba, E. S. Ali, and S. M. A. Elazim, "PI controller design for MPPT of photovoltaic system supplying SRM via BAT search algorithm," *Neural Comput. Appl.*, vol. 28, no. 4, pp. 651–667, Apr. 2017.
[26] A. S. Oshaba, E. S. Ali, and S. M. A. Elazim, "PI controller design using ABC algorithm for MPPT of PV system supplying DC motor pump load," *Neural Comput. Appl.*, vol. 28, no. 2, pp. 353–364, Feb. 2017.
[27] B. K. Verma and D. Kumar, "A review on artificial bee colony algorithm," *Int. J. Eng. Technol.*, vol. 2, no. 3, p. 175, Jun. 2013.
[28] W. Chen and Y. Xiao, "An improved ABC algorithm and its application in bearing fault diagnosis with EEMD," *Algorithms*, vol. 12, no. 4, p. 72, Apr. 2019.
[29] Y. Wu, B. Jiang, N. Lu, H. Yang, and Y. Zhou, "Multiple incipient sensor faults diagnosis with application to high-speed railway traction devices," *ISA Trans.*, vol. 67, pp. 183–192, Mar. 2017.
[30] R. Szczepanski, T. Tarczewski, and L. M. Grzesiak, "Adaptive state feedback speed controller for PMSM based on artificial bee colony algorithm," *Appl. Soft Comput.*, vol. 83, Oct. 2019, Art. no. 105644.
[31] J. C. Bansal, S. S. Jadon, R. Tiwari, D. Kiran, and B. K. Panigrahi, "Optimal power flow using artificial bee colony algorithm with global and local neighborhoods," *Int. J. Syst. Assurance Eng. Manage.*, vol. 8, no. 4, pp. 2158–2169, Dec. 2017.
[32] H. Gozde, M. C. Taplamacioglu, and I. Kocaarslan, "Application of artificial bee colony algorithm in an automatic voltage regulator (AVR) system," *Int. J. Tech. Phys. Problems Eng.*, vol. 1, no. 3, pp. 88–92, 2010.
[33] D. Oliva, E. Cuevas, and G. Pajares, "Parameter identification of solar cells using artificial bee colony optimization," *Energy*, vol. 72, pp. 93–102, Aug. 2014.
[34] L. Wang, X. Zhang, and X. Zhang, "Antenna array design by artificial bee colony algorithm with similarity induced search method," *IEEE Trans. Magn.*, vol. 55, no. 6, pp. 1–4, Jun. 2019.
[35] X. Zhang, X. Zhang, and L. Wang, "Antenna design by an adaptive variable differential artificial bee colony algorithm," *IEEE Trans. Magn.*, vol. 54, no. 3, pp. 1–4, Mar. 2018.
[36] S. Motahhir, A. El Hammoumi, and A. El Ghzizal, "The most used MPPT algorithms: Review and the suitable low-cost embedded board for each algorithm," *J. Cleaner Prod.*, vol. 246, Feb. 2020, Art. no. 118983.
[37] *High Efficiency Solar Battery Charger With Embedded MPPT*, document SPV 1040, ST Microelectronics, 2013.
[38] S. Padmanaban, N. Priyadarshi, M. S. Bhaskar, J. B. Holm-Nielsen, V. K. Ramachandaramurthy, and E. Hossain, "A hybrid ANFIS-ABC based MPPT controller for PV system with anti-islanding grid protection: Experimental realization," *IEEE Access*, vol. 7, pp. 103377–103389, 2019.
[39] J. Schönberger, "Modeling a photovoltaic string using PLECS, version 04-13," Plexim GmbH, Zürich, Switzerland, Tech. Rep., 2013.
[40] J. Chen, A. Prodic, R. W. Erickson, and D. Maksimovic, "Predictive digital current programmed control," *IEEE Trans. Power Electron.*, vol. 18, no. 1, pp. 411–419, Jan. 2003.
[41] C. Restrepo, T. Konjedic, F. Flores-Bahamonde, E. Vidal-Idiarte, J. Calvente, and R. Giral, "Multisampled digital average current controls of the versatile buck–boost converter," *IEEE J. Emerg. Sel. Topics Power Electron.*, vol. 7, no. 2, pp. 879–890, Jun. 2019.
[42] V. Tereshko, "Reaction-diffusion model of a honeybee colony's foraging behaviour," in *Proc. Int. Conf. Parallel Problem Solving Nature*. Berlin, Germany: Springer, 2000, pp. 807–816. [Online]. Available: https://citation-needed.springer.com/v2/references/10.1007/3-540-45356-3_79?format=bibtex&flavour=citation
[43] V. Tereshko and A. Loengarov, "Collective decision making in honey-bee foraging dynamics," *Comput. Inf. Syst.*, vol. 9, no. 3, p. 1, 2005.
[44] B. Nozohour-Leilabady and B. Fazelabdolabadi, "On the application of artificial bee colony (ABC) algorithm for optimization of well placements in fractured reservoirs; efficiency comparison with the particle swarm optimization (PSO) methodology," *Petroleum*, vol. 2, no. 1, pp. 79–89, Mar. 2016.
[45] M. H. Zafar, T. Al-shahrani, N. M. Khan, A. F. Mirza, M. Mansoor, M. U. Qadir, M. I. Khan, and R. A. Naqvi, "Group teaching optimization algorithm based MPPT control of PV systems under partial shading and complex partial shading," *Electronics*, vol. 9, no. 11, p. 1962, Nov. 2020.

CATALINA GONZÁLEZ-CASTAÑO received the degree in electronic engineering from the Universidad Nacional de Colombia, Manizales, in 2008, the M.Eng. degree in electrical engineering from the Universidad Tecnológica de Pereira, Colombia, in 2013, and the Ph.D. degree (Hons.) in electronic engineering, in the field of power converters for electric vehicles from the Universitat Rovira i Virgili, Tarragona, Spain, in 2019. She undertook her doctoral internship at the Advanced Center of Electrical and Electronic Engineering (AC3E), Valparaiso, Chile. Her main research interests include electric power quality, vehicular power systems, and design and digital control of power converters.

CARLOS RESTREPO received the bachelor's (Hons.) and master's degrees in electrical engineering from the Universidad Tecnológica de Pereira, Colombia, in 2006 and 2007, respectively, and the master's and Ph.D. (Hons.) degrees in electronic engineering from the Universitat Rovira i Virgili de Tarragona, Tarragona, Spain, in 2008 and 2012, respectively.

He was a Visiting Scholar with the Faculty of Electrical Engineering and Computer Science, University of Maribor, Slovenia, in 2011. From 2013 to 2014, he was a Postdoctoral Researcher with the Electrical Power Processing Group, Delft University of Technology, Delft, The Netherlands. From 2014 to 2016, he was a Professor with the Departamento de Ingeniería Eléctrica, Universidad Técnica Federico Santa María, Santiago de Chile, Chile. He is currently a Professor with the Departamento de Ingeniería Eléctrica, Universidad de Talca, Curicó, Chile. He is also the Director of the Laboratory of Applications in Smart Grids (LARI in Spanish) Research Group. His main research interests include modeling and emulator design for fuel cells, design and digital control of switched converters, and energy management of hybrid electric vehicles.

SAMIR KOURO (Senior Member, IEEE) received the M.Sc. and Ph.D. degrees in electronics engineering from the Universidad Tecnica Federico Santa Maria (UTFSM), Valparaiso, Chile, in 2004 and 2008, respectively. In 2007, he joined the Electronics Engineering Department, UTFSM, as a Research Associate, where he is currently a Professor. Since 2019, he has been the Director of innovation and technology transfer at UTFSM. He is a Founding Member and a Principal Investigator of the Solar Energy Research Center, Chile, and a Founding Member and the Deputy Director of the Advanced Center of Electrical and Electronics Engineering, Chile. His research interests include power electronics, renewable energy conversion systems (photovoltaic and wind), and electromobility. He was included in the 2018 Clarivate Analytics Highly Cited Researcher List. He was a recipient of the 2008 *IEEE Industrial Electronics Magazine* Best Paper Award, the 2012 IEEE Power Electronics Society Richard M. Bass Outstanding Young Power Electronics Engineer Award, the 2012 *IEEE Industry Applications Magazine* First Prize Paper Award, the 2012 IEEE Transactions on Industrial Electronics Best Paper Award, the 2015 IEEE Industrial Electronics Society J. David Irwin Early Career Award, and the 2016 IEEE Industrial Electronics Bimal K. Bose Award for Industrial Electronics Applications in Energy Systems.

JOSÉ RODRÍGUEZ (Life Fellow, IEEE) received the Engineer degree in electrical engineering from the Universidad Tecnica Federico Santa Maria, Valparaiso, Chile, in 1977, and the Dr.Ing. degree in electrical engineering from the University of Erlangen, Erlangen, Germany, in 1985. He has been with the Department of Electronics Engineering, Universidad Tecnica Federico Santa Maria, since 1977, where he was a Full Professor and the President. Since 2015, he has been the President with Universidad Andres Bello, Santiago, Chile, where he has been a Full Professor since 2019. He has coauthored two books, several book chapters, and more than 400 journal and conference papers. His main research interests include multilevel inverters, new converter topologies, control of power converters, and adjustable-speed drives. He has received a number of best paper awards from journals of the IEEE. He is a member of the Chilean Academy of Engineering. In 2014, he received the National Award of Applied Sciences and Technology from the Government of Chile. In 2015, he received the Eugene Mittelmann Award from the Industrial Electronics Society of the IEEE. From 2014 to 2019, he has been included in the list of Highly Cited Researchers published by Web of Science.